

QSAR Evaluation of the Ch'an Su and Related Bufadienolides against the Colchicine-Resistant Primary Liver Carcinoma Cell Line PLC/PRF/5¹

Yoshiaki Kamano,[†] Ayano Yamashita,[†] Toshihiko Nogawa,[†] Hiroshi Morita,[‡] Koichi Takeya,[‡] Hideji Itokawa,[‡] Toshiaki Segawa,[‡] Ayako Yukita,[§] Kyoko Saito,^{||} Mariko Katsuyama,^{||} and George R. Pettit^{*,[⊥]}

Faculty of Science, Kanagawa University, 2946 Tsuchiya, Hiratsuka, Kanagawa 259-1293, Japan; School of Pharmacy, Tokyo University of Pharmacy & Life Science, 1432-1 Horinouchi, Hachioji, Tokyo 192-0355, Japan; Tsukuba Institute, Toagousei Chemical Industry Co., 2 Ohkubo, Tsukuba, Ibaragi 300-2611, Japan; Sumisho Electronics Co., Ltd., 2-23 Shimomiyabi-cho, Shinjuku-ku, Tokyo 162-0822, Japan; and Cancer Research Institute and Department of Chemistry and Biochemistry, Arizona State University, Tempe, Arizona 85287-2404

Received May 13, 2002

QSAR analysis has been used to identify the essential structural requirements for increasing the inhibitory activities of selected bufadienolides from the Chinese drug Ch'an Su (and other sources) against the primary liver carcinoma cell line PLC/PRF/5 (PLC) and the derived colchicine-resistant line (COL). The variable substituent domain of the proposed pharmacophore of the bufadienolides was investigated using a Comparative Molecular Field Analysis (CoMFA) approach. A model with considerable predictive ability was obtained. In addition, the CoMFA results agreed well with the pharmacophore bufadienolide model for the parent PLC line proposed earlier.

Introduction

Various studies of the Chinese drug Ch'an Su²⁻⁶ and related bufadienolides^{3,4,7} have been conducted previously to better characterize possible inhibitors of cancer cell growth⁸⁻¹¹ and inducers of apoptosis,¹² and to study antiviral¹³ effects as well as the possibility of an endogenous mammalian bufadienolide being involved in Na⁺,K⁺-ATPase activity related to the pathogenesis of arterial hypertension.¹⁴⁻¹⁷ In our previous reports, the 3D structural features common to bufadienolides were characterized in respect to activity against the primary liver carcinoma PLC/PRF/5. The present study was designed to further evaluate the cancer cell growth inhibition of 74 bufadienolides and derivatives and six cardenolides against the colchicine-resistant primary liver carcinoma cell line PLC/PRF/5 abbreviated COL. A good SAR correlation was found between cancer cell growth inhibition against the parent (PLC) and resistant (COL) cell lines. That was followed by a series of studies that applied CoMFA methodology to rationalize the relationship between the 3D structures of the bufadienolides and their activities against the resistant cell line. The resulting model should provide reliable information for future drug design of anticancer bufadienolides.

Materials and Methods

Materials. Thin-plate Ch'an Su, which was a black rectangular thin plate (15 cm × 23 cm × 0.1 cm) prepared by Shanghai Medicinal Herbs Import and Export Corp. (Shanghai), was purchased in a Hong Kong folk-medicine market in

1995.¹⁸ Of the 80 compounds studied (Figures 1–5), some were isolated from Ch'an Su and others were obtained commercially or were bufadienolide derivatives prepared in our laboratories.

Bioassay. Primary liver carcinoma PLC/PRF/5 cells were maintained in tissue culture flasks, suitable cell suspensions were prepared, and 0.1 mL of the cell suspension was precultured in each well of the 96-well tissue culture plates for 24 h at 37 °C in a 5% CO₂ incubator. To these cells, colchicine was added to a concentration of 0.5 μg/mL. Next, one hundred microliters of appropriate dilutions of the test compounds (10⁻²-10⁻⁶ μg/mL) was added to each well, and the culture plates were further incubated (5% CO₂) for 72 h at 37 °C. Finally, the survival rate of the cells in the cultures was evaluated by the MTT method. The result was reported as IC₅₀, which is the concentration of test compound in μg/mL to give 50% inhibition of growth of the COL resistant cells.

Computational Methods.⁸ SYBYL molecular modeling software (ver 6.3) was used for all molecular modeling techniques and CoMFA studies. The compounds were built from fragments in the SYBYL database. Each structure was full geometry, optimized by using the standard Tripos molecular mechanics force field with a distance-dependent dielectric function and a 0.01 kcal/mol energy gradient convergence criterion. In addition, each stable conformer of side chains, including the δ-lactone ring at C-17, was obtained by using the systematic search routine in SYBYL. Partial atomic charges required for calculation of the electrostatic interaction energies were calculated by using the Gasteiger–Marsili method.

Calculations of ring centroids, least-squares fitting, and excluded volume analyses were also performed on the most active bufadienolides (IC₅₀ < 10⁻³, μg/mL) by using the Viatance Comparisons (DISCO) program in SYBYL. The pharmacophore mapping strategy was the calculation of the location of the ligand and site points, followed by execution of DISCO to find the pharmacophore maps. Other compounds were aligned via this pharmacophore model.

For each of the alignment sets, the steric and Coulombic potential energy fields were separately calculated at each lattice intersection on a regularly spaced grid of 2.0 ± units in all *x*, *y*, and *z* directions. The steric term represents the van der Waals interactions, whereas the Coulombic term repre-

* To whom correspondence should be addressed. Tel: 480-965-3351. Fax: 480-965-8558. E-mail: bpettit@asu.edu.

[†] Kanagawa University.

[‡] Tokyo University of Pharmacy & Life Science.

[§] Toagousei Chemical Industry Co.

^{||} Sumisho Electronics Co., Ltd.

[⊥] Arizona State University.

sents the electrostatic interactions for which a distance-dependent dielectric expression $\epsilon = R_{ij}$ was adopted. The grid pattern was generated automatically by the SYBYL/CoMFA routine. An sp^3 carbon atom with a +1.0 charge was selected as the probe for calculation of the steric and electrostatic field. Values of the steric and electrostatic energies were truncated at 30 kcal/mol.

To obtain a 3D QSAR, the partial least squares (PLS) method was used. The PLS method has been used successfully in many QSAR studies for rationalization of those structural features affecting biological activities. The PLS algorithm was initially used with the cross-validation option to obtain the optimal number of components needed for the subsequent analysis of the data. In the leave-one-out cross-validation, each compound was systematically excluded from the set and its activity predicted by a model derived from the rest of the compounds. The optimal number of components was then chosen as that which yielded either the smallest rms error or the largest cross-validated r^2 value. A final PLS analysis was then performed by using the reported optimum number of components, with no cross-validation. This generated a fitted correlation of the entire training set with conventional r^2 values. The steric and electrostatic fields were scaled according to the CoMFA standard deviations in order to give the same potential weights on the resulting QSAR. The 3D QSAR calibration model so derived was then employed to give theoretical inhibitory effect values for 10 bufadienolides which were then compared with their bioassay data.

Results and Discussion

Our study demonstrating the structure/cytotoxic activity/relationships (SAR) of these compounds is first summarized, followed by a compelling verification of this study wherein either the activities or molecular orientations were randomized and the CoMFA recalculated.

The inhibitory activities of 80 natural and related bufadienolides and cardenolides against the colchicine-resistant primary liver carcinoma cell line PLC/PRF/5 (COL) were measured using the MTT assay methods. The IC_{50} ($\mu\text{g/mL}$) values were determined (Table 1) and compared with those obtained using the parent cell line.^{8,9} Among the bufadienolides, the natural compounds showed a stronger activity than their derivatives. The most potent inhibitor was bufalin (**1**) which bears the 14β -OH, with an IC_{50} value of 2.8×10^{-4} $\mu\text{g/mL}$. The next strongest activities were exhibited by the cardenolide scillarenin (**11**), with a C-4 double bond, followed by the bufadienolides hellebrigenin (**19**) (19β -CHO), gamabufotalin (**15**) (11α -OH), and cinobufagin (**36**), each of which were in the IC_{50} range of 10^{-4} $\mu\text{g/mL}$ order. The 14β -hydroxy derivatives were generally more active than 14β , 15β -substituted compounds, α -pyrone ring-opened (weakest of all) compounds, and the other cardenolides.

For the resistant (colchicine) cell line PLC/PRF/5 evaluations, as done earlier^{8,9} with the PLC nonresistant line, the bufadienolides, cardenolides, and their derivatives were divided into Groups A–E: Group A, 14-hydroxy compounds (**1–20**, **60–62**); Group B, 14,15-epoxy compounds (**21–51**); Group C, cardenolides and derivatives (**63–68**); Group D, other bufadienolides (**52–59**); and Group E, derivatives with a cleaved α -pyrone ring (**69–80**). The SAR results revealed for each group may be summarized as follows.

Group A (1–20, 60–62) (Figure 1). The naturally occurring compounds showed strong activities compared to the derivatives. Compared to bufalin (**1**), introduction of 16β -acetoxy (**13**) and 16β -hydroxy (**14**) substituents

Table 1. Cancer Cell Growth Inhibition Shown by Bufadienolides and Related Derivatives against the Parent (PLC) and Resistant (COL) Cell Lines of PLC/PRF/5

no.	IC_{50} ($\mu\text{g/mL}$)		no.	IC_{50} ($\mu\text{g/mL}$)	
	PLC ^a	COL ^b		PLC ^a	COL ^b
1	2.8×10^{-4}	2.8×10^{-4}	41	6.4	9.8
2	7.6×10^{-2}	7.7×10^{-2}	42	5.6×10^{-2}	7.7×10^{-1}
3	2.0×10^{-4}	9.0×10^{-3}	43	7.8×10^{-1}	9.6
4	6.6×10^{-2}	5.1×10^{-1}	44	8.5×10^{-1}	5.6
5	5.9×10^{-2}	9.7×10^{-2}	45	2.4	7.6
6	7.5×10^{-4}	3.6×10^{-3}	46	5.2×10^{-1}	4.8
7	9.0×10^{-3}	9.4×10^{-2}	47	9.8×10^{-2}	3.4
8	6.2×10^{-4}	5.6×10^{-3}	48	50	>50
9	9.3×10^{-3}	6.1×10^{-1}	49	8.8×10^{-1}	1.0
10	7.5	21	50	1.0×10^{-3}	8.0×10^{-3}
11	3.1×10^{-4}	3.2×10^{-4}	51	6.7×10^{-1}	6.4×10^{-1}
12	1.9×10^{-4}	8.2×10^{-1}	52	7.0×10^{-2}	8.2×10^{-1}
13	3.4×10^{-4}	2.6×10^{-3}	53	8.2×10^{-1}	12
14	7.8×10^{-4}	8.0×10^{-3}	54	5.5×10^{-1}	1.8
15	2.3×10^{-4}	8.0×10^{-4}	55	8.2	12
16	6.0×10^{-2}	6.6×10^{-1}	56	7.0	10
17	7.9×10^{-1}	5.6	57	8.3×10^{-1}	9.0×10^{-1}
18	3.5×10^{-4}	2.6×10^{-3}	58	4.9	7.8
19	1.6×10^{-4}	5.3×10^{-4}	59	5.0	7.3
20	8.7×10^{-1}	6.8	60	35	30
21	8.9×10^{-3}	7.5×10^{-2}	61	7.1×10^{-1}	5.6
22	6.1×10^{-1}	8.2	62	7.7×10^{-2}	6.4
23	7.7×10^{-2}	7.6×10^{-2}	63	6.1×10^{-2}	7.5×10^{-1}
24	8.3	43	64	8.7×10^{-4}	9.2×10^{-3}
25	3.2×10^{-1}	9.5×10^{-1}	65	5.5×10^{-1}	5.0×10^{-1}
26	5.8	9.7	66	5.2	8.6
27	2.6	7.8	67	5.3×10^{-1}	9.8×10^{-1}
28	6.7	10	68	3.6×10^{-1}	7.3×10^{-1}
29	6.7	7.5	69	10	>50
30	20	26	70	9.1	45
31	4.7	6.4	71	6.6	41
32	8.7	43	72	7.5	9.5
33	5.9	7.3	73	6.4	41
34	4.7	43	74	49	50
35	5.2×10^{-1}	4.9×10^{-1}	75	9.7	20
36	7.4×10^{-4}	9.2×10^{-4}	76	9.5	>50
37	9.8×10^{-2}	9.0×10^{-1}	77	26	>50
38	4.0×10^{-2}	9.2×10^{-2}	78	>50	>50
39	8.5×10^{-1}	9.6×10^{-1}	79	8.4	>50
40	1.0×10^{-2}	6.0×10^{-2}	80	22	33

^a PLC: the activities against the parent PLC cell line ^b COL: the activities against the colchicine-resistant cell of PLC.

reduced the activity, whereas introduction of a double bond at C-4 (**11**), a 10β -aldehyde (**19**), and an 11α -hydroxy (**15**) made no significant difference in the degree of inhibition. However, conversion to the 3α -hydroxy and 3-ketone analogues lowered the potency as evident from comparison of compounds **1**, **2**, and **9**. Interestingly, bufalin 3-suberate (**6**) with its bulky ester showed stronger activities than the 3-succinate (**4**) derivative. Compared to **1**, which has the highest inhibitory activities, introduction of a 5β -hydroxy (**18**) lowered the effect.

Group B (21–51) (Figure 2). Cinobufagin (**36**) and derivatives showed strong inhibitory activities, but resibufogenin (**23**) and derivatives showed only moderate activities. Although substitution of an aldehyde (**21**) for the C-19 methyl of resibufogenin (**23**) kept the activity, insertion of a CH_2OH group (**22**) decreased the activity markedly. In this group, the introduction of ester (**25**, **38**, **39**, **40**, and **41**), ketone (**26** and **42**), and α -hydroxy (**24** and **37**) groups at the C-3 position led to weaker inhibitory activity compared to a β -hydroxy group (**23** and **36**). Introduction of a double bond at C-1

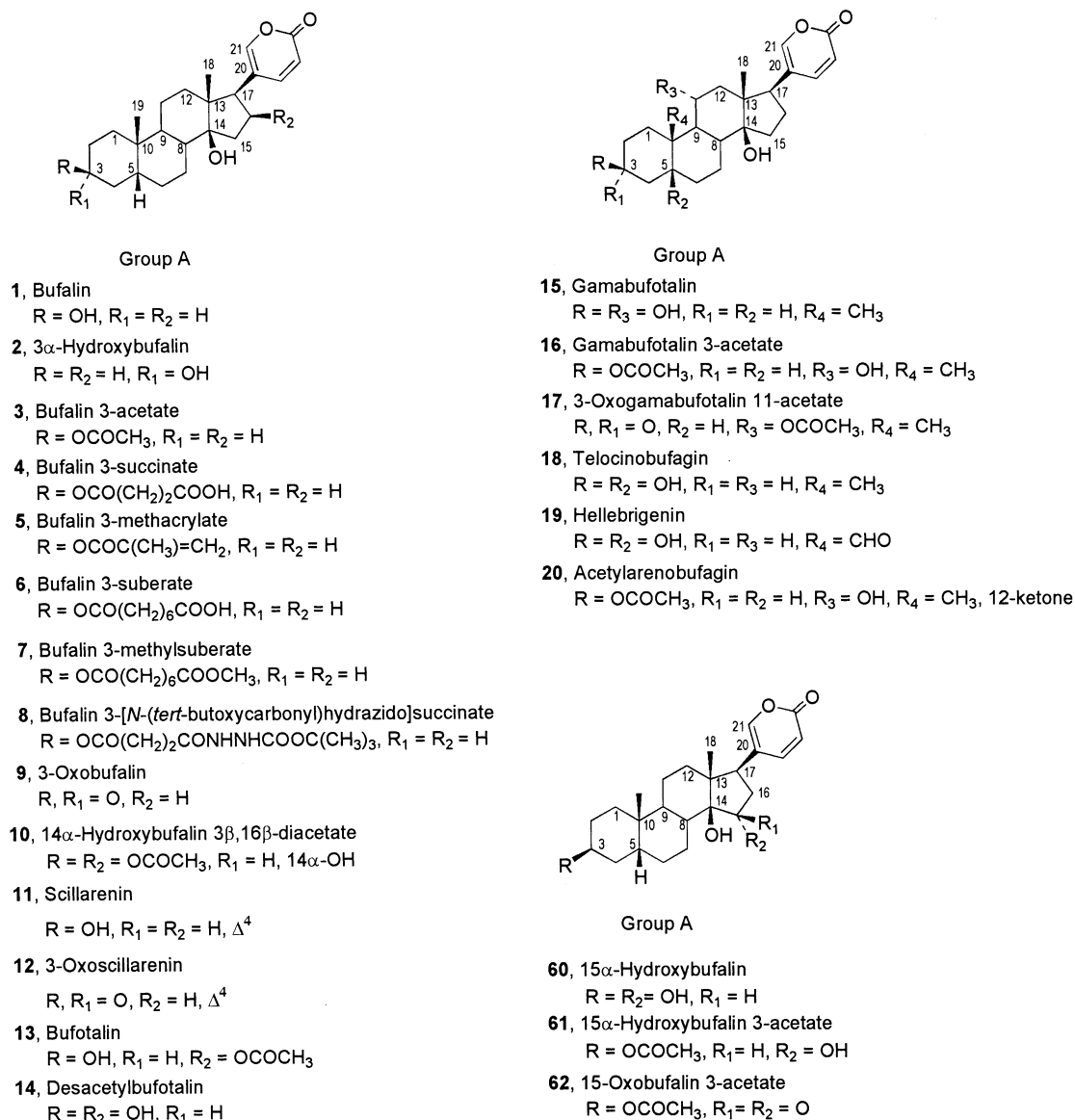


Figure 1. Structures of Group A bufadienolides 1–20 and 60–62.

or C-4 (27 or 28) is also unfavorable to activity. A 5 β -hydroxy group appears from two comparisons (50 and 36, 35 and 23) to have an unfavorable effect compared to a 5 β -proton. The presence of 14 β ,15 β -epoxy (23 and 35) and 16 β -acetoxy (36 and 50) groups at the D-ring increased the inhibitory activities compared to 14 α ,15 α -epoxy (30) and 16 β -hydroxy (46 and 51) groups. The presence of an acetoxy group in the C-16 position is a critical requisite for the activities. On the other hand, in Group A, the introduction of a 16 β -acetoxy group was an unfavorable factor.

Group C (63–68) (Figure 3). Cardenolides with their five-membered lactone ring at the C-17 β -position had moderate inhibitory activities compared to the bufadienolides with a six-membered α -pyrone ring. Digitoxigenin (64) showed the most favorable activities. The structure/activity relationships in Group C were similar to those of Group A.

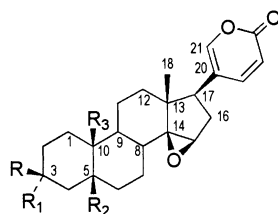
Group D (52–59) (Figure 4). The 14 β ,15 α -chlorohydrin (52) and Δ^{14} -bufalin (57) entries of Group D showed more potent inhibitory activity than those of Group E. The 14 α -artebufogenin (55) and 14 β -artebufogenin (53) proved to be comparably active.

Group E (69–80) (Figure 5). The existence of the bufadienolide α -pyrone ring is important for inhibitory activity.

The important structural features which influence the cancer cell growth inhibitory activities of the bufadienolides and related substances have been summarized in Figure 6. Interestingly, the results were the same as those found using the parent cell line PLC/PRF/5.⁸

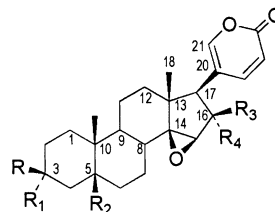
We next undertook a 3D QSAR interpretation using comparative molecular field analysis (CoMFA). The 3D QSAR techniques such as CoMFA have shown promise of providing useful extensions. By this means, a suitable sampling of the steric and electrostatic fields around a set of aligned structures provides information required for predicting the activities of untested structures. Therefore, we began with the program DISCO, following the development of a 3D QSAR model using CoMFA for the compounds originally used for 3D QSAR with the parent PLC/PRF/5 cell line.⁸

Next it was necessary to prepare a pharmacophore model to convert the 2D structures into 3D structures. Bufadienolides having potent cytotoxic activities ($IC_{50} < 10^{-3}$) were chosen as active compounds. On the basis



Group B

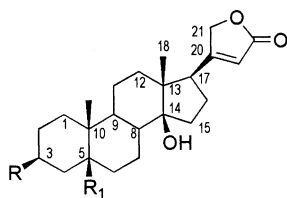
- 21, Resibufagin
R = OH, R₁ = R₂ = H, R₃ = CHO
- 22, Resibufaginol
R = OH, R₁ = R₂ = H, R₃ = CH₂OH
- 23, Resibufogenin
R = OH, R₁ = R₂ = H, R₃ = CH₃
- 24, 3 α -Hydroxyresibufogenin
R = R₂ = H, R₁ = OH, R₃ = CH₃
- 25, Resibufogenin 3-acetate
R = OCOCH₃, R₁ = R₂ = H, R₃ = CH₃
- 26, 3-Oxo-resibufogenin
R, R₁ = O, R₂ = H, R₃ = CH₃
- 27, $\Delta^{1,3}$ -3-Oxo-resibufogenin
R, R₁ = O, R₂ = H, R₃ = CH₃, Δ^1
- 28, $\Delta^{1,4}$ -3-Oxo-resibufogenin
R, R₁ = O, R₂ = H, R₃ = CH₃, Δ^1, Δ^4
- 29, 16 α -Hydroxyresibufogenin 3-acetate
R = OCOCH₃, R₁ = R₂ = H, R₃ = CH₃, 16 α -OH
- 30, 14 α ,15 α -Epoxyresibufogenin
R = OH, R₁ = R₂ = H, R₃ = CH₃, 14 α ,15 α -epoxy
- 31, 3 α -Hydroxy-14 α ,15 α -epoxyresibufogenin
R = R₂ = H, R₁ = OH, R₃ = CH₃, 14 α ,15 α -epoxy
- 32, 3-Oxo-14 α ,15 α -epoxyresibufogenin
R, R₁ = O, R₂ = H, R₃ = CH₃, 14 α ,15 α -epoxy
- 33, 14 α ,15 α -Epoxyresibufogenin 3-acetate
R = OCOCH₃, R₁ = R₂ = H, R₃ = CH₃, 14 α ,15 α -epoxy
- 34, 14 α ,15 α -Epoxyresibufogenin 3 α -acetate
R = R₂ = H, R₁ = OCOCH₃, R₃ = CH₃, 14 α ,15 α -epoxy
- 35, Marinobufagin
R = R₂ = OH, R₁ = H, R₃ = CH₃



Group B

- 36, Cinobufagin
R = OH, R₁ = R₂ = R₄ = H, R₃ = OCOCH₃
- 37, 3 α -Hydroxycinobufagin
R = R₂ = R₄ = H, R₁ = OH, R₃ = OCOCH₃
- 38, Cinobufagin 3-acetate
R = R₃ = OCOCH₃, R₁ = R₂ = R₄ = H
- 39, Cinobufagin 3-succinate
R = OCO(CH₂)₂COOH, R₁ = R₂ = R₄ = H, R₃ = OCOCH₃
- 40, Cinobufagin 3-suberate
R = OCO(CH₂)₆COOH, R₁ = R₂ = R₄ = H, R₃ = OCOCH₃
- 41, Cinobufagin 3-cinnamate
R = OCOCH=CHC₆H₅, R₁ = R₂ = R₄ = H, R₃ = OCOCH₃
- 42, 3-Oxocinobufagin
R, R₁ = O, R₂ = R₄ = H, R₃ = OCOCH₃
- 43, Cinobufagin 3-(3,5-dinitrobenzoate)
R = OCO[3,5-(NO₂)₂C₆H₃], R₁ = R₂ = R₄ = H, R₃ = OCOCH₃
- 44, 3,16-Diketocinobufagin
R, R₁ = O, R₂ = H, R₃, R₄ = O
- 45, 16-Oxocinobufagin 3-acetate
R = OCOCH₃, R₁ = R₂ = H, R₃, R₄ = O
- 46, Desacetylcinobufagin
R = R₃ = OH, R₁ = R₂ = R₄ = H
- 47, Desacetylcinobufagin 3-acetate
R = OCOCH₃, R₁ = R₂ = R₄ = H, R₃ = OH
- 48, Desacetylcinobufagin 3-acetate 16-succinate
R = OCOCH₃, R₁ = R₂ = R₄ = H, R₃ = OCO(CH₂)₂COOH
- 49, Desacetyl-14 α ,15 α -epoxycinobufagin 3-acetate
R = OCOCH₃, R₁ = R₂ = R₄ = H, R₃ = OH, 14 α ,15 α -epoxy
- 50, Cinobufotalin
R = R₂ = OH, R₁ = R₄ = H, R₃ = OCOCH₃
- 51, Desacetylcinobufotalin
R = R₂ = R₃ = OH, R₁ = R₄ = H

Figure 2. Structures of Group B bufadienolides 21–51.



Group C

- 63, Periplogenin R = R₁ = OH
- 64, Digitoxigenin R = OH, R₁ = H
- 65, Digitoxigenin 3-acetate R = OCOCH₃, R₁ = H
- 66, Digitoxigenin 3-suberate
R = OCO(CH₂)₆COOH, R₁ = H
- 67, Digitoxigenin 3-methylsuberate
R = OCO(CH₂)₆COOCH₃, R₁ = H
- 68, Δ^{14} -Digitoxigenin R = OH, R₁ = H, Δ^{14}

Figure 3. Structures of Group C cardenolides 63–68.

of chemical similarities such as hydrophobic or hydrogen-bond-donating or -accepting groups, the preferred con-

formers were examined in respect to the parent cell line (PLC) for their superimposability by the program DISCO. CoMFA analysis was performed for seventy of the natural compounds and derivatives by 'leave one out' cross-validation using the parent cell line, PLC. As a result, an acceptable q^2 (0.189) was obtained in this set. A second PLS analysis was performed by use of the optimum number of components with no cross-validation. The results of a noncross-validated PLS analysis using the 70 compounds are listed in Table 2, and the actual, predicted activities, and residuals are shown in Table 3. Clearly, the CoMFA-derived QSAR manifested a relatively good cross-validated r^2 and indicated thereby a considerable predictive and correlative capacity for growth inhibition of the colchicine-resistant cell lines. The ratio of steric and electrostatic contributions to the final model was 49:51. The relative contributions of the steric and electrostatic fields to this model were almost equal. Figure 7 shows the contribution of the steric and electrostatic fields to the CoMFA. The surfaces in Figure

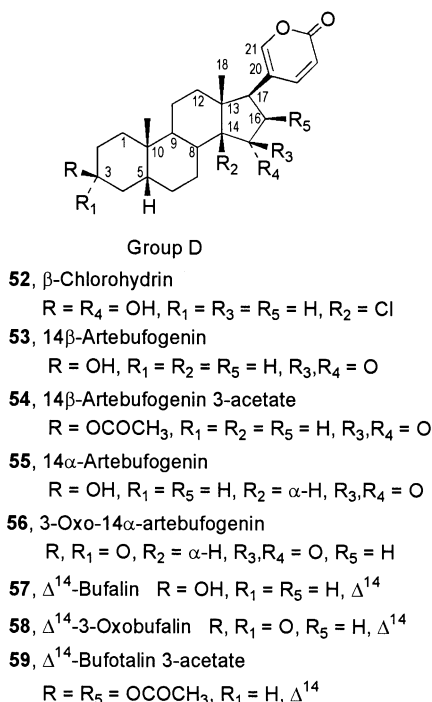


Figure 4. Structures of Group D bufadienolides **52–59**.

7 indicate the area in space around the template molecule (**6**). The contour map displays a region (colored green) where addition of steric bulk should be favorable and this region corresponds to the location of groups attached to C-14, -15, and -3 positions. In turn, this shows that the activities increased when bulky substituents were attached to these positions. Therefore, bulkier side substituents at C-14, -15 and -3 with the β -configuration enhances activities, suggesting that α -substitution at these positions leads to reduced activities. There are also three regions where steric bulk is contraindicated (colored yellow), namely, around the α -pyrone ring and the C-15 α -configuration.

In the electrostatic CoMFA map, a region (colored blue) where addition of positive charge would increase activities was identified below the α -face around the steroidal backbone skeleton and carbonyl moiety in α -pyrone ring. There is also a region (colored red) where addition of a negatively charged group should lead to increased activities. The regions of negative electrostatic interactions were scattered around the ester side chains at C-3 and C-5.

The preceding results provided a correlation between the inhibitory activities of these bufadienolides and the surrounding steric and electrostatic fields. The models obtained in this study are reasonably predictive, as indicated by the cross-validated r^2 values. The preceding conclusions indicate, in accord with the rationale for CoMFA, the interactions which seem most appropriate for evaluating the bufadienolides' cytotoxic activities against the colchicine-resistant cell line. A comparison now follows.

In general, as shown in Table 1, the compounds showing high inhibitory activities for the parent cell line of PLC also resulted in high activities against the resistant cell line (COL). The natural compounds showing high activities against the parent PLC cell line showed either similar or slightly weaker activities. Nine

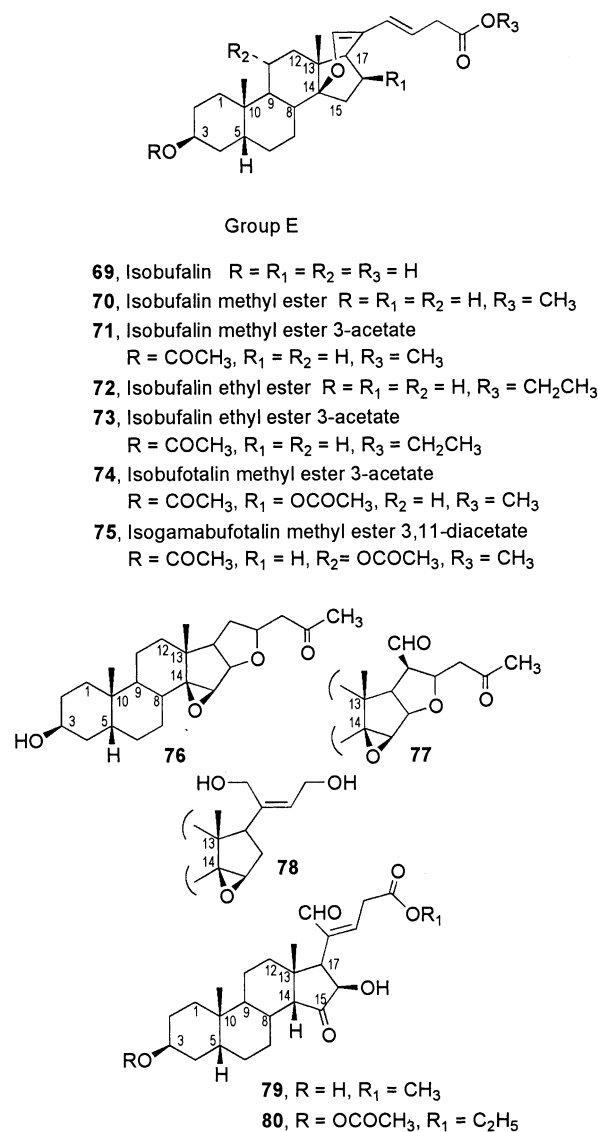


Figure 5. Structures of Group E with α -pyrone ring-opened modification (**69–80**).

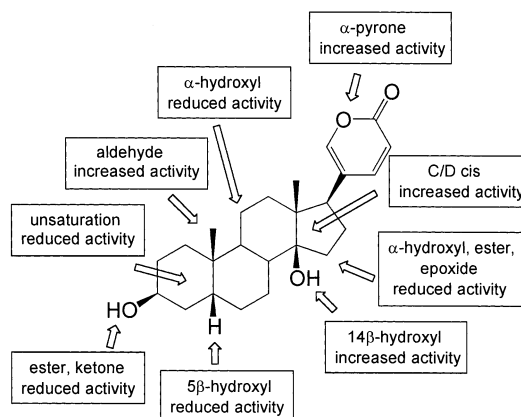


Figure 6. Effects of various structural modification of naturally occurring bufadienolides, cardenolides, and related derivation on inhibition of growth using the colchicine-resistant primary cancer cell line PLC/PRF/5 (COL). This structure is of bufalin (**1**).

of the naturally occurring bufadienolides and one of the cardenolides exhibited IC₅₀ values in the range 10⁻³ to

Table 2. Summary of CoMFA-PLS Results (COL cells)

no. of compounds	70
opt. no. of components	5
prob atom	$c(sp^3, +1)$
cross-validated r^2	0.189
std error of estimate	0.715
r^2	0.783
F values	46.105
contributions	
steric	0.494
electrostatic	0.506

Table 3. Actual and Predicted Activities and Residuals from CoMFA Analysis

compd	log 1/IC ₅₀ (PLC)						
	actual	predicted	residual	compd	actual	predicted	residual
1	3.55	1.93	1.62	41	-0.99	-0.77	-0.22
2	1.11	0.35	0.76	42	0.11	0.28	-0.16
3	2.05	0.85	1.20	43	-0.99	-0.98	-0.01
6	2.44	2.18	0.26	44	-0.75	-1.16	0.41
7	1.03	1.04	-0.02	45	-0.88	-0.92	0.04
9	0.22	0.20	0.02	46	-0.68	-0.99	0.30
10	-1.32	-1.25	-0.08	47	-0.53	-0.43	-0.10
11	3.49	2.74	0.76	49	0.00	-0.65	0.65
12	0.09	-0.04	0.13	50	2.10	2.01	0.08
13	2.59	3.10	-0.52	51	0.19	0.45	-0.26
14	2.10	2.08	0.02	52	0.09	0.50	-0.41
15	3.10	2.01	1.09	53	-1.08	-0.65	-0.43
16	0.18	0.92	-0.74	54	-0.25	-0.99	0.73
17	-0.75	-0.18	-0.56	55	-1.08	-0.86	-0.22
18	2.59	2.48	0.10	57	0.05	0.66	-0.62
19	3.28	3.08	0.20	58	-0.89	-1.14	0.25
20	-0.83	0.52	-1.35	59	-0.86	-0.07	-0.79
21	1.12	0.79	0.34	60	-1.48	1.18	-2.65
22	-0.91	-0.56	-0.35	61	-0.75	0.07	-0.81
23	1.12	-0.28	1.40	62	-0.81	-0.49	-0.31
24	-1.63	-1.09	-0.55	63	0.12	1.05	-0.92
25	0.02	-0.22	0.25	64	2.04	1.58	0.45
26	-0.99	-0.27	-0.72	65	0.30	0.02	0.29
29	-0.88	-0.68	-0.19	66	-0.93	-0.53	-0.40
30	-1.41	0.30	-1.72	68	0.14	-0.28	0.41
31	-0.81	-1.30	0.49	69	-1.70	-1.98	0.28
32	-1.63	-1.19	-0.44	70	-1.65	-1.60	-0.05
33	-0.86	-0.36	-0.50	71	-1.61	-1.98	0.37
34	-1.63	-2.32	0.69	72	-0.98	-1.78	0.80
35	0.31	-0.16	0.47	73	-1.61	-1.52	-0.09
36	3.04	1.70	1.33	74	-1.70	-1.18	-0.52
37	0.05	0.09	-0.04	75	-1.30	-1.69	0.39
38	1.04	0.52	0.51	78	-1.70	-1.67	-0.03
39	0.02	0.48	-0.47	79	-1.70	-1.77	0.07
40	0.22	0.39	-0.17	80	-1.52	-1.80	-0.28

10^{-4} $\mu\text{g/mL}$ against both the parent and resistant cells. The IC₅₀ values for these 10 compounds (see also Table 1) are as follows (parent PLC vs resistant): bufalin (**1**, 2.8×10^{-4} ; 2.8×10^{-4}), bufalin 3-acetate (**3**, 2.0×10^{-4} ; 9.0×10^{-3}), bufalin 3-suberate (**6**, 7.5×10^{-4} ; 3.6×10^{-3}), bufalin 3-[*N*-(*tert*-butoxycarbonyl)hydrazido]succinate (**8**, 6.2×10^{-4} ; 5.6×10^{-3}), scillarenin (**11**, 3.1×10^{-4} ; 3.2×10^{-4}), bufotalin (**13**, 3.4×10^{-4} ; 2.6×10^{-3}), desacetylbufotalin (**14**, 7.8×10^{-4} ; 8.0×10^{-3}), gamabufotalin (**15**, 2.3×10^{-4} ; 8.0×10^{-4}), telocinobufagin (**18**, 3.5×10^{-4} ; 2.6×10^{-3}), hellebrigenin (**19**, 1.6×10^{-4} ; 5.3×10^{-4}), cinobufagin (**36**, 7.4×10^{-4} ; 9.2×10^{-4}), cinobufotalin (**50**, 1.0×10^{-3} ; 8.0×10^{-3}), and digitoxigenin (**64**, 8.7×10^{-4} ; 9.2×10^{-3}).

Here it is noteworthy that most of the 80 compounds, including 10 previously synthesized compounds,⁸ showed activities against COL similar to or slightly weaker than those against the parent PLC. However, the inhibitions shown by 3-oxobufalin (**9**), 3-oxoscillarenin (**12**), 3 β -acetoxydesacetylbufotalin (**47**), and 3 β -acetoxy-15-

oxobufalin (**62**) against COL were significantly reduced compared with those against PLC. The natural bufadienolides bufalin (**1**), scillarenin (**11**), gamabufotalin (**15**), hellebrigenin (**19**), and cinobufagin (**36**) with IC₅₀s near 10^{-4} $\mu\text{g/mL}$ against PLC kept that potency against COL, whereas bufotalin (**13**), desacetylbufotalin (**14**), and telocinobufagin (**18**) showed somewhat reduced inhibitory activity against COL.

In all groups (A–E), the substituent effects against the COL line approximated those seen against the PLC line. In Group A, it's very interesting that bufalin (**1**) and scillarenin (**11**) showed high inhibitory activities against both PLC and COL cells, but 3-oxobufalin (**9**), 3-oxoscillarenin (**12**), and 3 β -acetoxy-15-oxobufalin (**62**) had low activities (IC₅₀ 6.1×10^{-1} , 8.2×10^{-1} , $6.4 \mu\text{g/mL}$) against COL cells, although they showed high activities (IC₅₀ 9.3×10^{-3} , 1.9×10^{-4} , $7.7 \times 10^{-2} \mu\text{g/mL}$) against PLC cells. Therefore, introduction of the 3-ketone was much less favorable against the COL line. With both the PLC and COL lines, introductions of 3 α -hydroxy or -ester, 5 α -hydroxy, 14 α -hydroxy, 15 α -hydroxy, and 16 β -hydroxy or -acetoxy typically reduced the activities.

In Group B, a 19-CHO group was found favorable for high potency, whereas a 19-CH₂OH group was less favorable for activities with both PLC and COL. Introduction of 16 β -hydroxy or -ester groups produced a marked drop in potency against both lines. Again, esterification or oxidation of a 3 β -hydroxy group greatly decreased activities.

Of Group C, digitoxigenin (**64**) showed the strongest inhibitory activity, but 3 β -acetoxydigitoxigenin (**65**) had greatly reduced activity against both lines as did other ester derivatives.

With Group D, the results suggested that oxygen at C-14 had a more important effect than other substituents. Except for Δ^{14} -bufalin (**57**), other C-14 modifications led to decreased activities against COL as compared to PLC. Since 14 β -artebufogenin (**53**) was 10 times more potent against PLC than 14 α -artebufogenin (**55**), it seems that the conformation of the D-ring arising from a *cis* C/D ring juncture is preferable for increased activity against PLC but in this series did not demonstrate enhancement against COL. Group E showed considerably weaker or no inhibition against the PLC and COL lines compared to the other groups. The SAR analysis of Groups A–E indicates that the 14 β -hydroxy group in bufadienolides is required for high inhibitory activities against the parent and resistant cell lines of PLC/PRF/5.

Results of the QSAR study using PLC showed a reasonable correlation with the SAR study.^{8,9} The steric effects around the C-, D-, and α -pyrone rings were similar for the PLC and COL lines, but the steric effects around C-3 did make a difference. With the parent PLC line steric bulk was contraindicated, but with the COL line steric bulk proved favorable for inhibition. The 3 β -suberate (**6** and **40**) derivatives of bufalin (**1**) and cinobufagin (**36**) appeared more active than the 3 β -succinate analogues against the resistant COL cell line. With electrostatic effects, no real differences were noted except with PLC where inhibitory activity increased when the electrostatic fields were positive around the α -pyrone ring. With the COL line, inhibition of growth

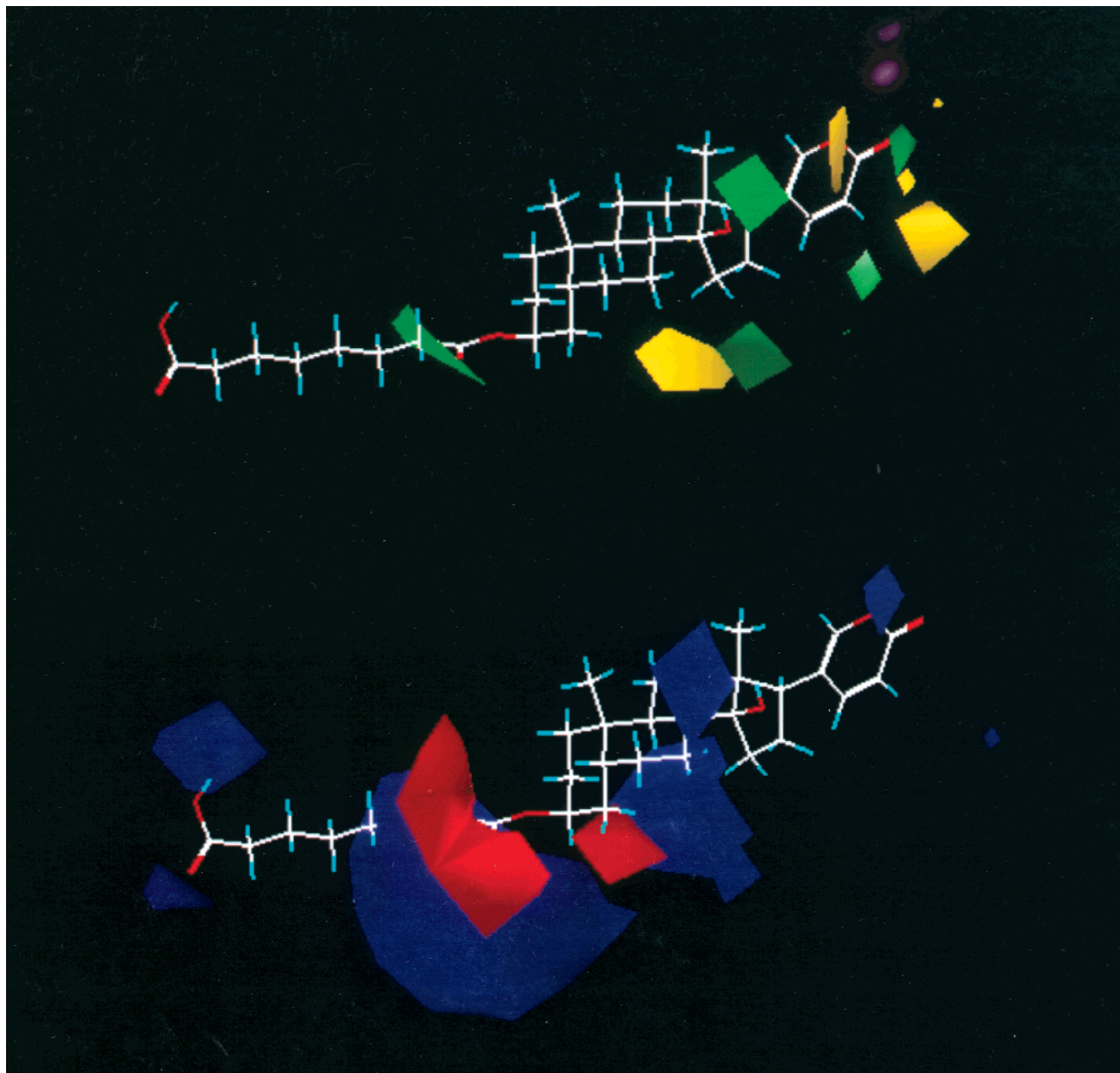


Figure 7. Stereoviews of CoMFA contour plots from the PLS analysis. Above: steric, below: electrostatic. Regions where increased steric bulk is associated with enhanced activity are indicated in green, whereas regions where increased steric bulk is associated with diminished activity are indicated in yellow. Regions where increased positive charge is favorable for activity are indicated in blue, whereas regions where increased negative charge is favorable are indicated in red.

increased when a negative electrostatic field was located in the α -pyrone ring region.

Conclusion

To be effective, an anticancer drug targeting liver cancer needs to potently inhibit both parent and resistant liver cancer cell lines. From the present SAR and QSAR analyses, it is evident that the naturally occurring bufadienolides and cardenolides generally showed the highest inhibition of the liver cancer cell lines PLC and COL compared to any of their derivatives. Particularly impressive were results from the nine naturally occurring bufadienolides [bufalin (**1**), scillarenin (**11**), bufotalin (**13**), desacetylbufotalin (**14**), gamabufotalin (**15**), telocinobufagin (**18**), hellebrigenin (**19**), cinobufagin (**36**), cinobufotalin (**50**)], three derivatives [3β -acetylbufalin (**3**), 3β -suberoylbufalin (**6**), bufalin 3β -[*N*-(*tert*-

butoxycarbonyl)hydrazido]succinate (**8**)], and one of the cardenolides, digitoxigenin (**64**). The mechanism of cancer cell growth inhibition evidenced by these bufadienolides needs to be further explored, and in vivo anticancer evaluations are needed. Such extended investigations will also include five new bufadienolides we recently isolated¹⁸ from Ch'an Su, which continues to be a remarkably important source of these biologically potent natural steroids.

Acknowledgment. We are pleased to thank the following for financial assistance: Outstanding Investigator Grant CA44344-12 and grant R01 CA90441-01 awarded by the Division of Cancer Treatment and Diagnosis, NCI, DHHS; the Arizona Disease Control Research Commission; the Fannie E. Rippel Foundation; Polly J. Trautman; John and Edith Reyno; Dr.

John C. Budzinski; the Ladies Auxiliary to the Veterans of Foreign Wars; and the Robert B. Dalton Endowment Fund.

References

- (1) For contribution 485, refer to: Pettit, G. R.; Collins, J. C., Knight, J. C., Herald, D. L., Williams, M. D., Pettit, R. K., Antineoplastic Agents 485. The Isolation and Structure of Cribrostatin 6, a Dark Blue Cancer Cell Growth Inhibitor from the Marine Sponge *Cribrochalina* sp. *J. Nat. Prod.*, in press.
- (2) Kamano, Y.; Kotake, A.; Nogawa, T.; Tozawa, M.; Pettit, G. R. Application of displacement thin-layer chromatography to toad-poison bufadienolides. *J. Planar Chromatogr.-Mod. TLC* **1999**, *12*, 120–123.
- (3) Kamano, Y.; Kotake, A.; Nogawa, T.; Hashima, H.; Tozawa, M.; Morita, H.; Takeya, K.; Itokawa, H.; Matsuo, I.; Ichihara, Y.; Drašar, P.; Pettit, G. R. Conformational preference of two toad poison bufadienolides, cinobufagin and bufotalin. *Collect. Czech. Chem. Commun.* **1998**, *63*, 1663–1670.
- (4) Kamano, Y.; Kotake, A.; Takano, R.; Morita, H.; Takeya, K.; Itokawa, H.; Pettit, G. R. Structure of the new alkaloids bufobutanoic acid and bufopyramide in Ch'an Su, and conformation of bufarenogin and Ψ -bufarenogin. *Tennen Yuki Kagobutsu Toronkai Koen Yoshishu* **1998**, *40*, 395–400.
- (5) Zhou, X.; Cheng, P.; Xu, M. Analytical methods of the constituents in Chansu. *Zhongcaoyao* **1992**, *23*, 490–494, 503.
- (6) Wang, J. D.; Narui, T.; Takatsuki, S.; Hashimoto, T.; Kobayashi, F.; Ekimoto, H.; Abuki, H.; Nijijima, K.; Okuyama, T. Hematological studies on naturally occurring substances. VI. Effects of an animal crude drug "Chan Su" (bufonis venenum) on blood coagulation, platelet aggregation, fibrinolysis system and cytotoxicity. *Chem. Pharma. Bull.* **1991**, *39*, 2135–2137.
- (7) Krenn, L.; Kopp, B. Bufadienolides from animal and plant sources. *Phytochemistry* **1998**, *48*, 1–29.
- (8) Kamano, Y.; Kotake, A.; Hashima, H.; Inoue, M.; Morita, H.; Takeya, K.; Itokawa, H.; Nandachi, N.; Segawa, T.; Yukita, A.; Saitou, K.; Katsuyama, M.; Pettit, G. R. Structure-cytotoxic activity relationship for the toad poison bufadienolides. *Bioorg. Med. Chem.* **1998**, *6*, 1103–1115.
- (9) Kamano, Y.; Kotake, A.; Hashima, H.; Abe, N.; Morita, H.; Itokawa, H.; Nandachi, N.; Zhang, H.; Ichihara, Y.; Kizu, H. Structures and antineoplastic activity of the toad poison bufadienolides. *Tennen Yuki Kagobutsu Toronkai Koen Yoshishu* **1996**, *38*, 9–354.
- (10) Lee, D. Y.; Yoon, H. J. Growth-inhibiting effect of bufadienolides on cultured vascular endothelial cells. *Korean J. Toxicol.* **1995**, *11*, 175–180.
- (11) Numazawa, S.; Shinoki, M.-A.; Ito, H.; Yoshida, T.; Kuroiwa, Y. Involvement of Na⁺, K⁺-ATPase inhibition in K562 cell differentiation induced by bufalin. *J. Cell. Physiol.* **1994**, *160*, 113–120.
- (12) Jing, Y.; Ohizumi, H.; Kawazoe, N.; Hashimoto, S.; Masuda, Y.; Nakajo, S.; Yoshida, T.; Kuroiwa, Y.; Nakaya, K. Selective inhibitory effect of bufalin and growth of human tumor cells in vitro: Association with the induction of apoptosis in Leukemia HL-60 cells. *J. Cancer Res.* **1994**, *85*, 645–651.
- (13) Nakanishi, T.; Nishino, H.; Ichiishi, E.; Mukainaka, T.; Okuda, M.; Tokuda, H. Inhibitory effects of bufadienolides on Epstein-Barr virus early antigen activation and on growth of mouse skin and mouse pulmonary tumors. *Nat. Med.* **1999**, *53*, 324–328.
- (14) Dmitrieva, R. I.; Bagrov, A. Y.; Lalli, E.; Sassone-Corsi, P.; Stocco, D. M.; Doris, P. A. Mammalian bufadienolide is synthesized from cholesterol in the adrenal cortex by a pathway that is independent of cholesterol side-chain cleavage. *Hypertension* **2000**, *36*, 442–448.
- (15) Antolovic, R.; Schoner, W. Is there an endogenous cardiac glycoside? *Herz/Kreislauf* **1999**, *31*, 15–20.
- (16) Doris, P. A.; Bagrov, A. Y. Endogenous sodium pump inhibitors and blood pressure regulation: an update on recent progress (44283). *Proc. Soc. Exp. Biol. Med.* **1998**, *218*, 156–167.
- (17) Bagrov, A. Y.; Fedorova, O. V.; Dmitrieva, R. I.; Howald, W. N.; Hunter, A. P.; Kuznetsova, E. A.; Shpen, V. M. Characterization of a urinary bufadienolide Na⁺, K⁺-ATPase inhibitor in patients after acute myocardial infarction. *Hypertension* **1998**, *31*, 1097–1103.
- (18) Nogawa, T.; Kamano, Y.; Yamashita, A.; Pettit, G. R. Isolation and Structure of Five New Cancer Cell Growth Inhibitory Bufadienolides from the Chinese Traditional Drug Ch'an Su. *J. Nat. Prod.* **2001**, *64*, 1148–1152.

JM0202066